

Enhancing Cellular Performance via Vehicular-based Opportunistic Relaying and Load Balancing

Saadallah Kassir*, Gustavo de Veciana*, Nannan Wang[†], Xi Wang[†] and Paparao Palacharla[†]

*The University of Texas at Austin, Electrical and Computer Engineering Department

[†]Fujitsu Laboratories of America, Richardson, TX

Abstract—The automotive industry is undergoing disruptive changes, e.g., ride sharing and self-driving cars which, in addition to leveraging wireless connectivity, may lead to dramatic changes in the volume of infotainment and work related data consumption of vehicle bound passengers. This paper studies the potential gains of leveraging clusters of V2V interconnected vehicles to enable: (1) improved opportunistic access to the cellular infrastructure; and (2), balancing traffic loads across cells through cluster multihoming. A stochastic geometric model and associated analysis are used to obtain a preliminary understanding of possible gains of cluster-based opportunistic relaying and its sensitivity to the system parameters, e.g., base station density, vehicular cluster size and density etc. An optimal network utility maximization formulation is then developed to serve as a baseline to evaluate a simple distributed cluster management algorithm which for the scenarios considered proves to be near-optimal. Overall the results suggest that 3-10x throughput gains are possible along with significant improvements in user rate fairness depending on the system parameters.

Index Terms—Vehicular Network, Vehicle-to-Vehicle Communication, Opportunism, Load Balancing

I. INTRODUCTION

Disruptive changes in automotive industry. The automotive industry is undergoing disruptive changes that are likely to have a significant impact on future wireless networks. These include: (1) the emergence and increasing usage of ride sharing fleets; (2) the expected development and adoption of driverless car technologies which may require robust vehicle-to-vehicle (V2V) and vehicle-to-infrastructure (V2I) connectivity; and (3) resulting shifts in the wireless traffic loads generated by commuters free to work/play while on the road. In this paper we embrace these changes by focusing on leveraging vehicular fleets to provide improved cellular connectivity to both vehicle-based and traditional mobile customers.

5G wireless landscape. Concomitant with changes in the automotive industry is the development of new technology for next generation 5G/6G wireless networks. In order to provide an effective platform to enable vehicles to enhance safety through collaborative sensing and/or maneuvering, real-time traffic data broadcasting, etc., the industry is envisaging the use of robust V2V communications going beyond DSRC, including high throughput (and ideally low latency) millimeter wave (mmWave) or visible light communications (VLC) as well as possibly integrated V2V+V2I connectivity. The "ubiquitous" availability of V2V connectivity offers the prospect of enabling new vehicle-based services, e.g., caching, that could also reduce the traffic loads on traditional cellular networks.

Vehicle cluster-based cooperative relaying. The focus of this paper is on how V2V+V2I architectures might be devised to address the key challenges cellular infrastructure will face, i.e., delivering high volumes of data to an increasing number of vehicular-based users. We consider a setting where clusters, or so called platoons, of well connected vehicles share possibly multi-homed connectivity to the cellular infrastructure. In other words one or more base stations (BSs) can transmit downlink data to a cluster of vehicles which can then relay data to appropriate destinations. This provides two classes of benefits which we discuss next.

Opportunistic throughput gains. The first type stems from the significant throughput gains achievable from opportunistic relaying to vehicle clusters. For example, as shown in Figure 1, rather than send directly to a vehicle v_4 at the cell edge, a BS b_1 can send data to a nearby vehicle v_1 and the cluster can then use high capacity V2V connectivity to relay data to v_4 . Given the order of magnitude differences in the peak capacity of nearby users compared to edge users in a typical cell, as long as V2V capacity is plentiful the potential of such cluster-based cooperative relaying is extremely high. When v_4 and v_1 lie in the same cell we refer to this as *intra-cell opportunism*, and if b_1 uses relay v_1 to forward data to a vehicle in another cell (say v_5) we call this *inter-cell opportunism*. This approach might be particularly relevant in mmWave based infrastructures, whose short range and susceptibility to obstructions make efficient deployment challenging. By leveraging cluster-based relaying one can exploit spatial diversity to find line of sight channels to BSs, providing improved coverage, throughput and reliability.

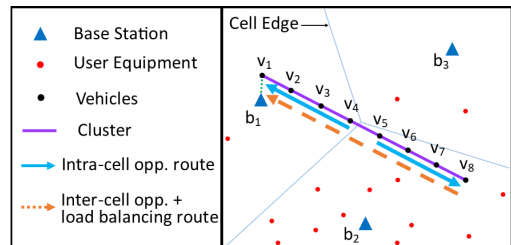


Fig. 1. Example of an 8 vehicle platoon traversing two BS cells shared by other mobile User Equipments (UEs).

Load balancing gains. The second type of benefit comes from enabling more flexible load balancing across neighboring cells. For example, as shown in Figure 1, the traffic destined to a cluster of vehicles spanning multiple BS cells, e.g., b_1

and b_2 , can be delivered through either one or both of the BSs, depending on the current cell loads. For instance, b_1 and b_2 currently have 5 and 15 users/vehicles in their respective cells but by using inter-cell cooperative relaying the loads could be shifted so that they each serve 9 and 11 respectively. Such an approach would help reducing the "peak-to-mean" cell load, hence diminishing the variability in users' perceived throughput. This is especially important in the context of 5G where small-cells cover limited regions and thus might see higher relative load variability.

Summary of paper objective. Different strategies can be devised to make the most of the aforementioned opportunistic and load balancing gains when exploiting cluster-based relaying. In general there is a tradeoff between opportunism and exploiting cluster multi-homing to balance loads, which has not been explored in prior work. While the mechanism underlying opportunism is naturally tied to the geometry (proximity) of clusters to neighboring BSs, that associated with load balancing is more subtle since 'optimal' decisions for clusters overlapping different subsets of cells will be coupled together across space. Below we discuss some of the related work in the literature.

Related work. Load balancing in cellular networks has been extensively studied especially in the context of heterogeneous networks. This includes a range of possible solutions, such as channel borrowing [1], cell breathing [2], BS association biasing [3], [4], or D2D based load balancing [5]–[7] and combinations thereof. Classical approaches include formalizing an optimization framework, see e.g., [6], [7] which in turn suggests appropriate scheduling algorithms, e.g., [5], [8], [9]. Recent studies have suggested learning based solutions to determine effective association policies, but perhaps lacks a development of underlying insights useful towards the design of vehicular networks, see e.g. [10]. Prior work has established the critical role that load balancing plays in improving mean user rate or some notion of fairness, see e.g., [11]. This work has certainly been extended to vehicular network settings where vehicles use V2I and V2V links to offload traffic from one cell to another [12]–[14]. While these works exhibit the benefits of load balancing, they focus on defining routing strategies, rather than analyzing the resource allocation problem and the potential per-user shared rate gains that an optimal load balancing scheme induces.

Another line of work has recently focused on studying multihomed load balancing schemes, e.g., [15] presents algorithms and experimental results showing how load balancing can improve the performance of multihop multihomed VANETs, but no network modeling and analysis was performed, and the study was mainly focused on the uplink access strategy, without discussing possible benefits for downlink.

Other studies have explored gains associated with relaying in cellular networks [16]–[18], commonly showing gains in throughput and fairness. For instance, [19] proposes a promising software framework that leverages opportunism to improve the total throughput delivered by a WiFi based WLAN network, improving it by a factor of two. Studies such as [20]

analyze the opportunistic gain in the context of VANETs, and also show that opportunism improves the downlink throughput. The focus is however on comparing the performance of three routing strategies, and proposing an efficient relay protocol rather than analyzing the gains associated with opportunism and load balancing. Although [20] analyzes an RSU-based network, it still provides some valuable insight regarding exploiting opportunism.

Paper's contributions and organization. The main contribution of this paper lies in quantifying the potential benefits of vehicle cluster based opportunistic relaying in terms of per-user throughput gains as well as improved fairness, i.e., reduced throughput variability resulting from load balancing. A study of the effects that variations in the network parameters have on the network performance gains is presented to complement the results.

To that end in Section II we propose a stochastic geometric model and in Section III the associated analysis geared at understanding intra-cell opportunistic gain's sensitivity to the system parameters. In Section IV we introduce an optimal network utility maximization formulation which captures both intra- and inter-cell opportunistic and load balancing gains and serves as a baseline to evaluate a simple distributed cluster management algorithm proposed in Section V. Section VI includes both numerical and simulation results for a variety of scenarios suggesting 3-10x throughput gains along with significant improvements in fairness depending on the system parameters. Finally Section VII concludes the paper.

II. SYSTEM MODEL

In this section we propose a model enabling us to analytically evaluate possible intra-cell opportunistic gains for cluster-based cooperative relaying.

A. Network Model

We consider a network wherein BSs are randomly placed on the plane according to a Poisson Point Process (PPP) $\Phi_{BS} = \{B_i : i \in \mathbb{N}\}$ with intensity λ_{BS} , see e.g., [21]. Another independent PPP $\Phi_{UE} = \{U_i : i \in \mathbb{N}\}$ with intensity λ_{UE} models the locations of other users User Equipment (UE), also referred as *mobile users*. Vehicle clusters are modeled as randomly located linear platoons having a random number of vehicles. Specifically, the clusters' centers are located according to a third independent PPP $\Phi_C = \{C_i : i \in \mathbb{N}\}$ with intensity λ_C . Each cluster C_i has an independent random number of vehicles $M_i \sim \text{Geom}(\mu)$ and which are placed with equal spacing (distance d_v) on a randomly oriented line. μ is set to be equal to $e^{-\lambda_v d_v}$, corresponding to V2V cluster models arising when vehicles are located as a PPP process of intensity λ_v on the roads. Note that in reality cluster orientations would be coupled along roads but for simplicity we will consider the above setting. The above vehicle cluster model induces a (non Poisson) point process $\Phi_V = \{V_i : i \in \mathbb{N}\}$ denoting the locations of the vehicles in the network. Each vehicle is assumed to also correspond to an active user.

In the sequel we let $\phi_{\text{BS}} = \{b_i : i \in \mathbb{N}\}$ denote a realization of the PPP Φ_{BS} and refer to BSs directly through and their locations, e.g., b_i . This convention is adopted for all point processes. As shown in Figure 2, the BSs ϕ_{BS} induce a Voronoi tessellation $\mathcal{T}(\phi_{\text{BS}}) = \{\mathcal{T}^b(\phi_{\text{BS}}) \mid b \in \phi_{\text{BS}}\}$, where each BS b has an associated cell

$$\mathcal{T}^b(\phi_{\text{BS}}) = \{x \in \mathbb{R}^2 \mid \|x - b\|_2 \leq \|x - b'\|_2, \forall b' \in \phi_{\text{BS}}\}.$$

Based on this tessellation of BS's cells we define the following additional notation. The set of vehicles $\phi_{\mathcal{V}}$ is partitioned such that \mathcal{V}_c denotes vehicles belonging to cluster c while \mathcal{V}^b denotes the set of vehicles in BS b 's cell. Finally, the set of mobile UEs ϕ_{UE} in the network is partitioned such that \mathcal{U}^b denotes the set of UEs in BS b cell. Assuming UEs and vehicles associate with their closest BS, we have that $n_{b,\text{UE}} = |\mathcal{U}^b|$, $n_{b,\mathcal{V}} = |\mathcal{V}^b|$ and $n_b = n_{b,\text{UE}} + n_{b,\mathcal{V}}$ denote the number of UEs, vehicles and total users associated with b .

Note since the inter-vehicular distance is fixed to d_v , and the random cluster size is $M \sim \text{Geom}(\mu)$ vehicles the cluster length L in meters is given by

$$p_L(l \cdot d_v) = \mu(1 - \mu)^l, l = 0, 1, 2, \dots, \quad (1)$$

where we have assumed the convention that a cluster with one vehicle has length 0, with two vehicles length d_v and so forth.

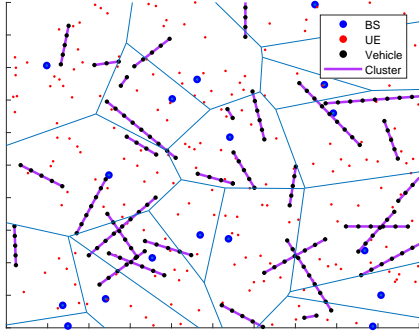


Fig. 2. Network Model

B. Connectivity and Link Capacity Model

In our analysis we only consider *downlink* transmissions. For the *traditional cellular* network the downlink transmission capacity to mobile user u (or similarly vehicle v) associated to BS b depends on the SINR given by

$$\text{SINR}_u^b = \frac{H_u^b p \|b - u\|_2^{-\alpha}}{I_u^b + \sigma^2}, \quad (2)$$

where $H_u^b \sim \text{Exp}(1)$ models random fading from BS b and user u , p is the BS transmission power, $\|b - u\|_2$ is the distance from b to u , α is the path-loss coefficient, σ^2 models noise in the system, and finally I_u^b is the interference a transmission from b to u sees from other BSs, i.e.,

$$I_u^b = \sum_{b' \in \phi_{\text{BS}} \setminus \{b\}} H_u^{b'} p \|b' - u\|_2^{-\alpha} \quad (3)$$

We model the downlink transmission capacity based on the Shannon rate, i.e.,

$$r_u^b = WE[\log(1 + \text{SINR}_u^b)] \quad (4)$$

where W represents the system bandwidth and the expectation is taken over channel fadings for a given realization of the BSs and user/vehicle locations. In this setting the transmission capacity to vehicles is determined in a similar way. Finally we shall assume each BS b allocates an equal fraction of time/frequency resources to each user/vehicle in its cell, i.e., associated with it. Thus we define the *shared* Shannon rate from BS b to an associated user (or vehicle) as

$$s_u^b = \frac{1}{n_b} r_u^b = \frac{1}{n_b} WE[\log(1 + \text{SINR}_u^b)]. \quad (5)$$

In our model for network leveraging *cluster-based opportunistic relaying* UEs see the same shared rate as our traditional cellular network model. By contrast the transmission rate from BS b to an associated vehicle v belonging to cluster c , i.e., a vehicle $v \in \mathcal{V}_c \cap \mathcal{V}^b$, is modeled by

$$r_v^{b,*} = \max_{v' \in \mathcal{V}_c \cap \mathcal{V}^b} r_{v'}^b \quad (6)$$

i.e., the highest rate achievable from b to a (relay) vehicle in the *same* cell and vehicle cluster as v —thus only *intra-cell* opportunism is considered. We shall further make the following assumption which is in line with a setting where vehicles use high capacity V2V line of sight links, e.g., mmWave.

Assumption 1. We assume intra-cluster V2V links have sufficiently high capacity as to ensure they do not bottleneck in relaying downlink traffic to vehicles within clusters, and do not interfere with infrastructure transmissions.

Thus, under this assumption in the cooperative setting the achievable shared rate for a vehicle $v \in \mathcal{V}_c \cup \mathcal{V}^b$ is given by

$$s_v^{b,*} = \frac{1}{n_b} r_v^{b,*} = \frac{1}{n_b} \max_{v' \in \mathcal{V}_c \cap \mathcal{V}^b} r_{v'}^b. \quad (7)$$

This initial model does not capture the impact of *inter-cell* opportunistic relaying and load balancing to be considered in more detail in the sequel.

III. PERFORMANCE ANALYSIS

In this section we develop analytical expressions for the two network settings introduced in Section II. The aim is to capture the key role that geometry plays and its impact on the achievable intra-cell opportunism gains.

A. Traditional Cellular Network

We shall consider the performance as seen by a *typical*¹ mobile or vehicular bound user in a traditional cellular network setting. Let (R, N) be random variables whose joint distribution corresponds to that of a typical user's downlink Shannon rate and the number of users sharing its BS, so the mean typical user's shared Shannon rate S is given by

$$E[S] = \mathbb{E} \left[\frac{R}{N} \right] \approx \mathbb{E}[R] \cdot \mathbb{E} \left[\frac{1}{N} \right], \quad (8)$$

¹A typical user here refers to a randomly selected user.

where the approximation has been found to be quite accurate, see e.g., [22], and expected to be a lower bound given R and $\frac{1}{N}$ might be surmised to be positively correlated, i.e., a low value for R likely reflects a large cell, which would tend to have a larger number of users, and thus also a low value $\frac{1}{N}$. The following theorem based on standard arguments, see Appendix, provides a characterization of our traditional cellular network serving a mix of mobile and vehicular cluster-based users.

Theorem 1. *For a typical user in the traditional cellular network the distance D to its closest BS satisfies*

$$f_D(d) = 2\pi\lambda_{BS}de^{-\lambda_{BS}\pi d^2}, \forall d \geq 0 \quad (9)$$

and its mean downlink Shannon rate is given by

$$\mathbb{E}[R] = \int_{\mathbb{R}_+^3} P(I_d \leq \frac{hpd^{-\alpha}}{e^r - 1} - \sigma^2) f_D(d) f_H(h) d d d h d r \quad (10)$$

where $H \sim \text{Exp}(1)$ and I_d is a random variable representing the conditional distribution for the interference given $D = d$ with MGF $M_{I_d}(t) = \exp(-2\pi\lambda_{BS} \int_d^\infty \frac{x}{1-(tp)^{-1}x^\alpha} dx)$.

Furthermore assuming $A \sim \text{Gamma}(3.5, \frac{3.5}{\lambda_{BS}})$ models the area of a randomly selected cell (see [23]) we have that

$$\mathbb{E}\left[\frac{1}{N}\right] \geq \frac{\lambda_{BS}[1 - M_A(-(\lambda_{UE} + \lambda_C))] }{\lambda_{UE} + \lambda_C E[M]} \quad (11)$$

$$\mathbb{E}\left[\frac{1}{N}\right] \leq \frac{\lambda_{BS}[1 - M_A(-(\lambda_{UE} + \lambda_C E[M]))]}{\lambda_{UE} + \lambda_C E[M]} \quad (12)$$

where $M_A(t) = E[e^{At}] = (1 - \frac{3.5}{\lambda_{BS}}t)^{-3.5}$.

B. Vehicular Cluster-based Opportunistic Relaying

Next we characterize the shared rate of a typical user in a setting with vehicle cluster-based intra-cell opportunistic relaying. Paralleling the analysis for the traditional cellular network, for a typical *vehicular-based* user we let R^* denote downlink Shannon rate to the best possible opportunistic relaying (within its cluster and associated cell) and let N^* denote the number of users sharing its BS's cell. Note that $N^* \sim N$ and that the Shannon rate to a typical mobile user remains the same as in Theorem 1.

Figure 3(a) exhibits the geometry of vehicular cluster-based opportunistic relaying. The distance between a typical vehicle and its closest BS D still has the distribution in Eq. (9). This is denoted by a line segment between the origin (BS) and a vehicle at a distance $D = d$ away on the x -axis. The typical vehicle also belongs to a cluster of length L^* whose distribution corresponds to the length biased distribution of L given in Eq. (1), i.e., typical vehicles are more likely to belong to longer clusters, so $p_{L^*}(l \cdot d_v) = \frac{l \cdot d_v \cdot p_L(l d_v)}{\mathbb{E}[L]}$ for $l = 0, 1, \dots$. In the figure the cluster is denoted by a line segment of length $L^* = l^*$ whose intersection with the x -axis corresponds the typical vehicles location in its cluster. For our typical vehicle, we model the orientation of its cluster (acute angle) as $\Theta \sim \text{Unif}[0, \frac{\pi}{2}]$ which is independent of the typical vehicle's cluster length L^* and distance D . This is denoted by $\Theta = \theta$ in the figure.

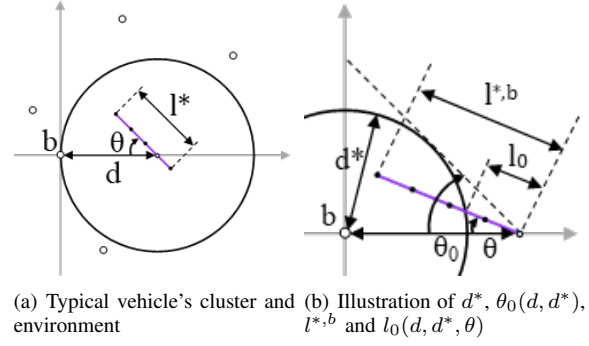


Fig. 3. Geometry of vehicle cluster based opportunistic relaying

The location of a typical vehicle within its cluster is uniformly distributed, and "breaks" the cluster into two pieces. We denote by $L^{*,b}$ the length of the cluster pointing in the direction of the BS, i.e., $L^{*,b} = l^{*,b}$ i.e., where there may be candidate opportunistic relays with better channels to the BS at the origin. The distribution of $L^{*,b}$ is shown in the Appendix to be:

Lemma 1. $L^{*,b}$ is such that $L^{*,b} \sim L$ given in Eq. (1).

To capture cluster-based opportunistic gains we need to determine D^* the minimum distance between a relay vehicle on the cluster segment of length $L^{*,b}$ and BS with the additional requirement that the relay vehicle also belongs to the typical vehicles cell. This requires the absence of any other BSs within a disc of radius D around the typical vehicle and any other BSs within a disc of radius D^* around the relaying vehicle. In the figure we show a possible realization of $D^* = d$. Note that $D^* \leq D$ almost surely, since a typical vehicle can of course receive data directly from its associated BS. This is where opportunistic relay gains come from.

Figure 3(b) exhibits the definition of two key functions of the geometry: (1) $\theta_0(d, d^*)$ the angle of the tangent to a disc of radius d^* , and (2) $l_0(d, d^*, \theta)$ which for $\theta \leq \theta_0(d, d^*)$ is the length of the segment starting from $(d, 0)$ with angle θ to the disc of radius d^* . With these definitions one can evaluate

$$P(D^* > d^*) = \sum_{i=1}^3 \int_{d^*}^\infty P(D^* > d^*, \mathcal{E}_i | D = d) f_D(d) dd. \quad (13)$$

if $d > d^*$, and $P(D^* > d) = 0$ otherwise; by identifying a partition $\mathcal{E}_1, \mathcal{E}_2$ and \mathcal{E}_3 corresponding to the three cases/events exhibited in Figure 4 and given by

- Case 1: $\mathcal{E}_1 = \{\Theta > \theta_0(d^*, D)\}$
- Case 2: $\mathcal{E}_2 = \{\Theta \leq \theta_0(d^*, D), L^{*,b} < l_0(D, d^*, \Theta)\}$
- Case 3: $\mathcal{E}_3 = \{\Theta \leq \theta_0(d^*, D), L^{*,b} \geq l_0(D, d^*, \Theta)\}$

Theorem 2. *For a typical UE in the network with intra-cell opportunistic relaying, the same results as in Theorem 1 hold. For a typical vehicle, the distance D^* between the best vehicle relay in its cluster and its associated BS satisfies is given by Eq. (13) where the three terms in the summation are explicitly worked out in Eqs. (32), (34) and (38). Further, the mean rate*

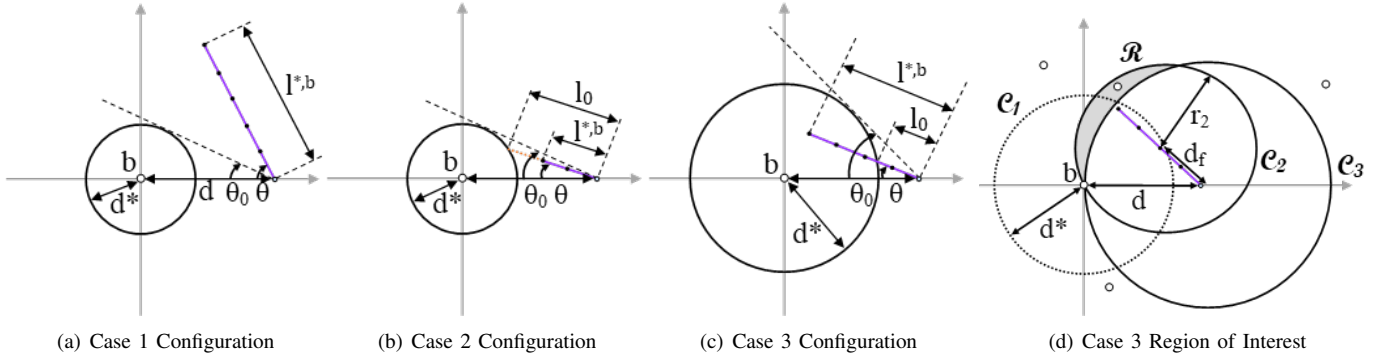


Fig. 4. Typical Vehicle's Cluster Configuration Analysis

seen by a typical vehicle satisfies

$$\mathbb{E}[R^*] \geq \int_{\mathbb{R}_+^3} P(I_d \leq \frac{hpd^{-\alpha}}{e^r - 1} - \sigma^2) f_{D^*}(d) f_H(h) dddhdr \quad (14)$$

where H and I_d are as in Theorem 1. The number of users N^* sharing the BS with a typical user (mobile or vehicle) is such that $N^* \sim N$ satisfying the bounds in Eqs. (11) and (12).

Figure 5 exhibits the expected shared rate evaluation of these expressions as a function of λ_C , and comparing them to simulation results. The simulation parameters are presented in Table I. We use a relatively high value of α set to be 5, to model the path loss of mmWave signals for V2I links, that has been validated experimentally [24]. The theoretical plots show the derivations to be relatively tight lower bounds to the actual expected shared rate seen by a typical vehicle. We note that the lower-bound proposed in Eq. (11) has been used to generate Figure 5, but both bounds are very tight for these parameters, effectively resulting in the same plot.

TABLE I
NETWORK SIMULATION PARAMETERS

Parameter	Value	Units
λ_{BS}	3e-6	BSS/m ²
λ_{UE}	3e-5	UEs/m ²
λ_v	20e-3	vehicles/m
d_v	50	m
d_r	150	m
α	5	-
p/σ^2	1e10	-

As can be seen in the figure, cooperative relaying leads to considerable gains in per-user shared rate. An improvement by a factor of $4\times$ for this specific scenario in the expected shared rate seen by a typical vehicle, only considering opportunism. Our next step is to propose a distributed algorithm performing load balancing, and compare its performance against those results.

IV. JOINT OPTIMIZATION OF OPPORTUNISTIC RELAYING AND BASE STATION LOAD BALANCING

In this section we consider the joint optimization of opportunistic relaying and load balancing so as to fairly allocate BSs' resources amongst a set of mobile and vehicle bound

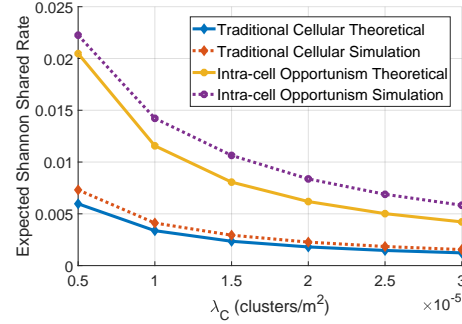


Fig. 5. Theoretical bounds and simulations for the per-user shared rate for a traditional cellular network and one leveraging intra-cell opportunism

users. The proposed *centralized* optimization problem is used to motivate and evaluate the performance of a simple algorithm discussed in Section V.

We will formulate our optimization framework for users in a finite region $\mathcal{X} \subset \mathbb{R}^2$. To that end we adopt the same notation as in Section II but restricted to BSs, users, clusters, and vehicles in the region \mathcal{X} which are denoted by $\mathcal{B}, \mathcal{U}, \mathcal{C}, \mathcal{V}$ respectively. Further for any BS b we let \mathcal{C}^b denote the set of clusters that include *at least one* vehicle in b 's cell, and \mathcal{V}_c the set of vehicles in cluster c . We let \mathcal{B}^c denote the set of BSs which contain at least one of cluster c 's vehicles in its cell.

As in Section II, we shall assume that BS $b \in \mathcal{B}$ serves the set of mobiles \mathcal{U}^b in its Voronoi cell, such that for $u \in \mathcal{U}^b$ the downlink transmission capacity is r_u^b given in Eq. (4). Similarly we denote as \mathcal{V}^b the set of vehicles in the BS b cell. However, in contrast, the set of vehicles which b can serve via cluster relaying is denoted $\mathcal{V}^{b,*}$ where

$$\mathcal{V}^{b,*} = \cup_{c \in \mathcal{C}^b} \mathcal{V}_c \quad (15)$$

which may include vehicles which are not in b 's cell. For each $v \in \mathcal{V}^{b,*} \cap \mathcal{V}_c$ we define the effective downlink transmission capacity from b to v as

$$r_v^{b,*} = \max_{v' \in \mathcal{V}_c \cap \mathcal{V}^b} r_{v'}^b \quad (16)$$

i.e., the highest rate b can deliver to vehicle v is by relaying through a vehicles in v 's cluster that are *also* in b 's cell. This additional flexibility for a BS b to possibly serve vehicles in

other cells is at the core of the ability of our cluster-based cooperative relaying mechanism to improve load balancing.

For each mobile and vehicle bound user w in the network we posit a concave utility function $U_w(\cdot)$ of its allocated rate ρ_w . For example, if $U_w(\rho_w) = \log(\rho_w)$ such allocations are referred to as *proportionally fair* [25]. The key decision variables are $\boldsymbol{\pi} = (\pi^b : b \in \mathcal{B})$ where $\pi^b = (\pi_w^b : w \in \mathcal{U}^b \cup \mathcal{V}^{b,*})$, which represents the fraction of BS b 's allocated to the mobiles and vehicles it can serves. thus

$$\|\boldsymbol{\pi}^b\|_1 = \sum_{w \in \mathcal{U}^b \cup \mathcal{V}^{b,*}} \pi_w^b = 1. \quad (17)$$

With this notation in place the network utility optimization problem is given as follows

$$\begin{aligned} \max_{\boldsymbol{\pi}} \quad & \sum_{w \in \mathcal{U} \cup \mathcal{V}} U_w(\rho_w) \\ \text{s.t.} \quad & \rho_u = \pi_u^b r_u^b \quad \forall u \in \mathcal{U}^b, \forall b \in \mathcal{B}, \\ & \rho_v = \sum_{b \in \mathcal{B}_c} \pi_v^b r_v^{b,*} \quad \forall v \in \mathcal{V}_c, \forall c \in \mathcal{C}, \\ & \|\boldsymbol{\pi}^b\|_1 = 1, \boldsymbol{\pi}^b \geq 0 \quad \forall b \in \mathcal{B}. \end{aligned} \quad (18)$$

Note that while mobile users can only be served by one BS, vehicular based users can be *multihomed*, i.e., served by multiple BSs which opportunistically relay their data through other vehicles in their cluster.

The above optimization problem is convex but may not have a unique optimizer [26]. Intuitively if there were a cycle of BSs linked by overlapping vehicle clusters it may be possible to shift resource allocations around the cycle while maintaining the same overall network utility. In practice this also requires particular conditions in the BSs loads and downlink transmission capacity to users. In the sequel we solve the above optimization to evaluate the effectiveness of the simpler resource allocation algorithm proposed next.

V. VEHICLE CLUSTER MULTI-HOMING FOR COOPERATIVE RELAYING ALGORITHM

In this section we propose a simple decentralized algorithm for vehicle cluster management. Given the expected dynamics of vehicular clusters relative to the BSs, simplicity is highly desirable. The idea is to have clusters initiate updates to their relationships with the BS infrastructure at random times or when substantial changes have arisen, e.g., a "handoff." Let us first consider a static setting and for simplicity suppose all mobile and vehicle-based users are to be treated equally. Using the notation introduced in the previous section, each cluster c will periodically update how many² of its set \mathcal{V}_c of vehicle based users should be served by each of the BSs \mathcal{B}_c the cluster currently overlaps.

In particular let $\mathbf{n}^c = (n_b^c : b \in \mathcal{B}_c)$ where n_b^c denotes the number of cluster c vehicles served by BS b , and where $\|\mathbf{n}^c\|_1 = |\mathcal{V}_c|$. Let $\mathbf{m}^c = (m_b^c : b \in \mathcal{B}_c)$ where m_b^c denotes the number of *other* mobiles and vehicle based (i.e., excluding cluster c) users BS b is currently serving. Finally with a slight

²Recall we have assume V2V capacity amongst vehicles in the cluster is not a bottleneck, hence we will not focus on which vehicles, though a natural approach would be one that minimizes the V2V load on the cluster.

abuse of notation we shall define $\mathbf{r}^c = (r_c^b : c \in \mathcal{B}_c)$ where r_c^b denotes the highest transmission rate BS b can achieve amongst cluster c vehicles in its cell, note for any $v \in \mathcal{V}_c$ we have $r_c^b = r_v^{b,*}$ defined earlier.

When the cluster management update is engaged, it takes the current \mathbf{m}^c and \mathbf{r}^c and determines $\mathbf{n}^{c,*}$ such that

$$\mathbf{n}^{c,*} = \arg \max_{\mathbf{n}^c} \min_{b \in \mathcal{B}_c} \frac{r_c^b}{n_b^c + m_b^c} \quad (19)$$

i.e., it greedily maximizes its vehicle users minimum rate allocation, based on local information only. Note the above assumes each BS allocates an equal fraction of time to each of its UEs and vehicles.

As a final step, the vehicles in \mathcal{V}_c aggregate their resources in a common pool and redistribute them uniformly among themselves, in such a way that all the vehicles in a cluster perceive similar QoS.

Also note that determining $\mathbf{n}^{c,*}$ is a straightforward task of computational complexity $O(|\mathcal{B}_c||\mathcal{V}_c|)$. Finally assuming BSs track m_b^c and r_c^b the information requirement to perform a cluster update is $O(|\mathcal{B}_c|)$.

In summary, in our proposed algorithm, clusters management updates are triggered by either a necessary handoff or after a random time out. A handoff would arise if for example there were a change in \mathcal{V}_c or \mathcal{B}_c , e.g., due to the clusters' motion a BS is no longer able to serve c . Cluster updates continue adapting to changes in base stations mobile user loads and vehicle dynamics. However in our simulations presented in the next section, we consider only randomly generated but static network configurations.

VI. RESULTS AND PERFORMANCE EVALUATION

We evaluated network performance for random network configurations based on the network parameters shown in Table I. Four different settings were considered:

Traditional cellular: all users associate with their closest BS which shares its resources equally amongst them.

Intra-cell opportunism: setting analyzed in Section II where only cluster-based intra-cell opportunism was exploited.

Network optimal: corresponds to solving the centralized network utility maximization Problem (18) introduced in Section IV where all users have log utilities, i.e., proportionally fair resource allocation.

Distributed algorithm: refers to the algorithm described in Section V where initial allocations were based on BSs only serving vehicles in their cells and then cluster rebalancing updates conducted. The number of such updates was three times the number of vehicles in the simulated area, the updated clusters were selected at random.

Note that only the last two exploit both intra and inter-cell opportunism and load balancing. Two metrics were used to compare the networks performance: (1) the mean per user-shared rate, and (2) Jain's fairness index for users' shared rate allocations.

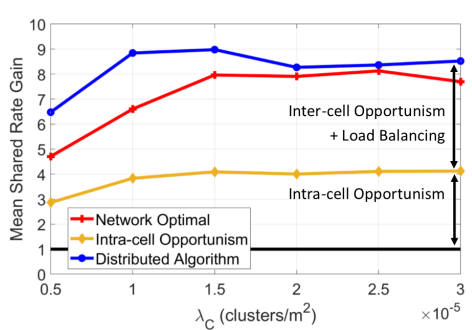


Fig. 6. Simulated Network Mean-Rate Gain Performance of the Network Optimal ($k_v = k_u = 1$), Intra-cell Opportunism and Distributed Algorithm, with respect to the Traditional Cellular scenario performance

A. Mean Per-User Shared Rate

Figure 6 exhibits the gains in the per-user mean shared rate achieved in each setting relative to the traditional cellular network, as a function of increased vehicle cluster density λ_C . This captures both increased network congestion and load balancing flexibility. We observe that the distributed algorithm performs better than the network optimal allocations reaching gains up to $9\times$ and $8\times$ respectively. In retrospect this is not surprising because, as shown in Figure 7, the network optimal allocations are more fair. Another observation is the performance benefits of inter-cell opportunism and load balancing, improving gains from $4\times$ to $9\times$, i.e., roughly doubling the gains realized when only intra-cell opportunism is used. Finally we note that the gains are roughly increasing in λ_C , with higher increases in lightly loaded networks. This results from increased BS activity each with more users nearby and increased but saturating benefits of inter-cell load balancing.

B. Fairness in per user rate allocations

Rather than use the achieved network utility to evaluate fairness, we used the Jain's index [27] metric that offers the advantages of being continuous, population size and metric independent, but perhaps more importantly bounded between 0 and 1 respectively representing the least and most fair allocations. As can be seen in Figure 7, the distributed algorithm and network optimal allocations greatly improve fairness as compared to traditional cellular setting. The network optimal allocations are the most fair, benefiting from the global network view, versus the distributed algorithm which uses only local information. Once again we observe that a considerable amount of improvement in fairness appears to be due to exploitation of inter-cell opportunism and load balancing. In fact the impact on fairness of such flexibility appears to be higher than that on the mean per-user shared rate; it contributes to more than half of the total "fairness gain". Finally we note that fairness under network optimal and the distributed algorithm increases in λ_C reflecting the increased inter-cell load balancing flexibility that such clusters enable.

C. Parameter Sensitivity Analysis

To get a deeper understanding of the impact of the simulation parameters on the gains, we explored their sensitivity

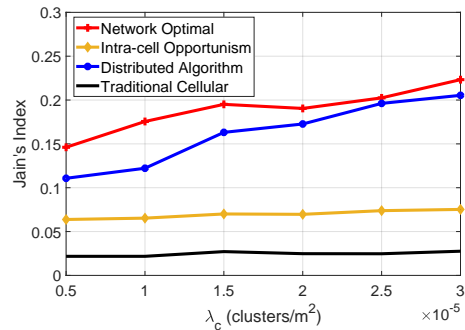


Fig. 7. Simulated Jain's Index of the Fairness Optimal ($k_v = k_u = 1$), Intra-cell Opportunism, Distributed Algorithm and Traditional Cellular Scenarios

to various changes. First, a change of path-loss coefficient α from 5 to 4, for $\lambda_c = 20$ clusters/km², reduced per user rate gains from $8\times$ down to $3\times$ but these are still considerable gains. One can expect settings where path loss is high (e.g., mmWave) to benefit more from the proposed techniques.

Second we increased λ_v resulting in increased cluster sizes. We observed that intra-cell opportunism saturates quickly, since eventually longer clusters do not help. By contrast, the gains from inter-cell opportunism and load balancing gain keep increasing, even exceeding $10\times$ for $\lambda_v = 30$ vehicles/km.

Lastly we consider the impact of λ_{BS} . As the BS density increases we found that the gains from intra-cell opportunism drop since users tend to be closer to their BS, and the opportunistic gains of relay through other vehicles in the same cluster may be marginal. However, the inter-cell and load balancing gain still increases as BSs benefit from the flexibility of balancing loads. This effect is somewhat weaker than opportunistic gains leading to reduced overall gains.

VII. CONCLUSIONS

In this work, we studied the gains associated with inter-vehicular communication, and focused on understanding the role played by both opportunism and load balancing. We presented an analytical framework based on our network model to derive expressions for the mean shared-rate perceived by a typical user in the network, and validated the derivations using simulations. We then established an optimization framework to associate users to BSs and allocate the wireless resources fairly, and used it as a benchmark to analyze the performance of our proposed simple, efficient, and distributed algorithm. Results show that associating V2V to V2I leads indeed to mean user rate and fairness gains, coming from both opportunism and load balancing with roughly equivalent impact, and that satisfactory performance can be reached using our proposed algorithm.

REFERENCES

- [1] S.K. Das, S.K. Sen, and R. Jayaram. A dynamic load balancing strategy for channel assignment using selective borrowing in cellular mobile environment. *Wireless Networks*, 3, October 1997.
- [2] A. Sang, X. Wang, M. Madhian, and R.D. Gitlin. A load-aware handoff and cell-site selection scheme in multi-cell packet data systems. In *Proc. IEEE GLOBECOM*, volume 6, December 2004.

- [3] Q. Ye et. al. User association for load balancing in heterogeneous cellular networks. *IEEE Trans. Wireless Comm.*, 12, June 2013.
- [4] A. Sharma, A. Trivedi, and N. Roberts. Efficient load balancing using D2D communication and biasing in LTE-advance het-nets. In *Proc. IEEE ICCT*, September 2015.
- [5] H. Zhang, L. Song, and Y.J. Zhang. Load balancing for 5G ultra-dense networks using device-to-device communications. *IEEE Trans. Wireless Comm.*, 17, June 2018.
- [6] L. Deng et. al. Device-to-device load balancing for cellular networks.
- [7] C. Saha and H. Dhillon. D2D underlaid cellular networks with user clusters: Load balancing and downlink rate analysis. In *Proc. IEEE WCNC*, March 2017.
- [8] S. Das, H. Viswanathan, and G. Rittenhouse. Dynamic load balancing through coordinated scheduling in packet data systems. In *Proc. IEEE INFOCOM*, volume 1, April 2003.
- [9] J. Liu et.al. Device-to-device communications achieve efficient load balancing in LTE-advanced networks. *IEEE Trans. Wireless Comm.*, 21, April 2014.
- [10] Z. Li, C. Wang, and C.-J. Jiang. User association for load balancing in vehicular networks: An online reinforcement learning approach. *IEEE Trans. Intel. Transp. Systems*, 18, August 2017.
- [11] L. Le and E. Hossain. Multihop cellular networks: Potential gains, research challenges, and a resource allocation framework. *IEEE Comm. Mag.*, 45, September 2007.
- [12] T.P. Van. Location-aware and load-balanced data delivery at road-side units in vehicular ad hoc networks. In *IEEE Consumer Electronics (ISCE)*, June 2010.
- [13] D. Wu et. al. Geographic load balancing routing in hybrid vehicular ad hoc networks. In *IEEE Intell. Transp. Systems*, October 2011.
- [14] B. Sliwa, R. Falkenberg, and C. Wietfeld. A simple scheme for distributed passive load balancing in mobile ad-hoc networks. *arXiv preprint arXiv:1702.05235*, February 2017.
- [15] F. Castro et. al. Multihoming for uplink communications in vehicular networks. In *Wireless Days*, March 2017.
- [16] H. Wu et. al. Integrated cellular and ad hoc relaying systems: iCAR. *IEEE JSAC*, 19, October 2001.
- [17] J. Cho and Z.J. Haas. On the throughput enhancement of the downstream channel in cellular radio networks through multihop relaying. *IEEE JSAC*, 22, September 2004.
- [18] C.-H. Yu and O. Tirkkonen. Opportunistic multiple relay selection with diverse mean channel gains. *IEEE Trans. Wireless Comm.*, 11, March 2012.
- [19] P. Bahl et. al. Opportunistic use of client repeaters to improve performance of w lans. *IEEE/ACM Trans. Networking*, 17, August 2009.
- [20] J. Yoo, B. Choi, and M. Gerla. An opportunistic relay protocol for vehicular road-side access with fading channels. In *Proc. IEEE ICNP*, October 2010.
- [21] J. G. Andrews, A. Gupta, and H. Dhillon. A primer on cellular network analysis using stochastic geometry. *CoRR*, October 2016.
- [22] P. Madadi, F. Baccelli, and G. de Veciana. Shared rate process for mobile users in poisson networks and applications. *IEEE Trans. Info. Theory*, 64, March 2018.
- [23] J.-S. Ferenc and Z. Néda. On the size distribution of poisson voronoi cells. *Physica A: Statistical Mechanics and its Applications*, 385, November 2007.
- [24] Y. Azar et. al. 28 ghz propagation measurements for outdoor cellular communications using steerable beam antennas in new york city. In *Proc. IEEE ICC*, June 2013.
- [25] T. Lan et. al. An axiomatic theory of fairness in network resource allocation. In *Proc. IEEE INFOCOM*, March 2010.
- [26] B. Hajek. Balanced loads in infinite networks. *Ann. App. Prob.*, 6, 1996.
- [27] R.K. Jain, D.-M. Chiu, and W.R. Hawe. A quantitative measure of fairness and discrimination. *Eastern Research Laboratory, Digital Equipment Corporation*, September 1984.
- [28] J. Andrews, F. Baccelli, and R.K. Ganti. A tractable approach to coverage and rate in cellular networks. *IEEE Trans. Comm.*, 59, November 2011.
- [29] M. Haenggi et. al. Stochastic geometry and random graphs for the analysis and design of wireless networks. *IEEE JSAC*, 27, September 2009.
- [30] B. Blaszczyzyn and D. Yogeshwaran. On comparison of clustering properties of point processes. *Ann. App. Prob.*, 46, March 2014.
- [31] Eric W. Weisstein. Circle-circle intersection. *MathWorld*—<http://mathworld.wolfram.com/Circle-CircleIntersection.html> (Online).

APPENDIX

Proof. (Theorem 1) The expression for $\mathbb{E}[R]$ for the traditional cellular setting is standard, see e.g., [28], we nevertheless outline the argument as it will be needed to develop the cooperative relaying result. The typical user's SINR depends on D, H and the interference I so by conditioning we get:

$$\begin{aligned}\mathbb{E}[R] &= \mathbb{E}[\ln(1 + \text{SINR})] = \int_0^\infty P(\ln(1 + \frac{HpD^{-\alpha}}{\sigma^2 + I}) \geq r) dr \\ &= \int_{\mathbb{R}_+^3} P(\ln(1 + \frac{hpd^{-\alpha}}{\sigma^2 + I_d}) \geq r | D = d, H = h) \\ &\quad f_D(d)f_H(h) dddh dr \\ &= \int_{\mathbb{R}_+^3} P(I_d \leq \frac{hpd^{-\alpha}}{e^r - 1} - \sigma^2) f_D(d)f_H(h) dddh dr\end{aligned}\quad (20)$$

where $H \sim \text{Exp}(1)$ and where D and I_d have well known distributions [28], [29]:

$$f_D(d) = 2\pi\lambda_{\text{BS}}de^{-\lambda_{\text{BS}}\pi d^2}, \forall d \geq 0, \quad (21)$$

$$M_{I_d}(t) = \exp(-2\pi\lambda_{\text{BS}} \int_d^\infty \frac{x}{1 - (tx)^{-1}x^\alpha} dx) \quad (22)$$

Let us now consider $\mathbb{E}[\frac{1}{N}]$. The distribution for the number of users N sharing with a typical user can be related to that of the number of users on a typical BS N_b by

$$p_N(n) = \frac{n \cdot p_{N_b}(n)}{\mathbb{E}[N_b]}, \quad (23)$$

capturing the sampling bias for a typical user being more likely to be in a cell with more users. This in turn gives that

$$\mathbb{E}\left[\frac{1}{N}\right] = \frac{1}{\mathbb{E}[N_b]} \cdot (1 - p_{N_b}(0)). \quad (24)$$

Further given the stationarity of the point process of mobile and vehicle-based users the mean number of users in a typical BS's cell is spatial density of users times the mean area of a cell, i.e., $\mathbb{E}[N_b] = (\lambda_{\text{UE}} + \lambda_c \mathbb{E}[M]) \cdot \frac{1}{\lambda_{\text{BS}}}$.

Let $A \sim \text{Gamma}(3.5, \frac{3.5}{\lambda_{\text{BS}}})$ be a random variable whose distribution is known to model the area of a typical cell, see e.g., [23]. Recall that for a typical cell $N_b = N_{b,\text{UE}} + N_{b,\text{V}}$ and that given $A = a$ we have that $N_{b,\text{UE}}$ and $N_{b,\text{V}}$ are conditionally independent so

$$p_{N_b}(0) = \int_0^\infty P(N_{b,\text{UE}} = 0 | A = a) P(N_{b,\text{V}} = 0 | A = a) f_A(a) da \quad (25)$$

Furthermore $p_{N_{b,\text{UE}}|A}(\cdot|a) \sim \text{Poisson}(\lambda_{\text{UE}}a)$ so

$$P(N_{b,\text{UE}} = 0 | A = a) = e^{-\lambda_{\text{UE}}a}. \quad (26)$$

By contrast the positive correlations in vehicle locations due to the cluster model result in a weakly super-PPP for vehicle locations [30] so

$$P(N_{b,\text{V}} = 0 | A = a) \geq e^{-\lambda_c \mathbb{E}[M]a}. \quad (27)$$

Also one can show a trivial upper bound

$$P(N_{b,\text{V}} = 0 | A = a) \leq e^{-\lambda_c a} \quad (28)$$

by considering the probability that no cluster center hits a cell of area a . Using this the above upper bound we obtain

$$p_{N^*}(0) \leq \int_0^\infty e^{-(\lambda_{UE} + \lambda_C)a} f_A(a) da = M_A(-(\lambda_{UE} + \lambda_C)). \quad (29)$$

giving the result in the theorem, and the lower bound is similarly obtained. \square

Proof. (Lemma 1) We know that $M \sim \text{Geom}(\mu)$. A typical vehicle will see a size biased cluster size M^* whose distribution is given by $p_{M^*}(m) = \frac{m \cdot p_M(m)}{\mathbb{E}[M]}$. A typical vehicle location within its cluster is be uniformly distributed, thus $M^{*,b}$ be the number of vehicles in the remaining part of the typical vehicle's cluster. Since the typical vehicle is uniformly distributed among the M^* possible positions, $p_{M^{*,b}|M^*}(m^b|m) = \frac{1}{m}, \forall m^b \leq m$. Hence,

$$p_{M^{*,b}}(m^b) = \sum_{j=m^b}^\infty p_{M^{*,b}|M^*}(m^b|j) p_{M^*}(j) = \mu(1-\mu)^{m^b-1}. \quad (30)$$

Thus $M^{*,b} \sim M$ and it follows that $L^{*,b} \sim L$ given in Eq. (1). \square

Proof. (Theorem 2) We consider the three cases in (13).

Case 1. For a given d, d^* the angle of the tangent is given by

$$\theta_0(d, d^*) := \sin^{-1}(d^*/d) \quad (31)$$

and note from Figure 4(a) that if $\Theta \geq \theta_0(d, d^*)$ then the cluster does not hit the radius d^* disc, whence $D^* \geq d^*$. Since Θ is uniformly distributed between 0 and $\pi/2$, the first integral term corresponding to \mathcal{E}_1 in Eq. (13) is given by

$$\int_{d^*}^\infty \frac{\pi/2 - \theta_0(d^*, d)}{\pi/2} f_D(d) dd \quad (32)$$

Case 2. For a given d, d^* and $\theta < \theta_0(d, d^*)$ note from Figure 4(b) that a cluster extending a length $L^{*,b}$ such that

$$L^{*,b} \leq l_0(d, d^*, \theta) := d \cos(\theta) + \sqrt{d^{*2} - (d \sin(\theta))^2} \quad (33)$$

will not hit the disc of radius d^* ensuring that $D^* > d^*$. Here $l_0(d, d^*, \theta)$ is determined by a triangle of side lengths l_0, d and d^* , knowing θ . The second integral term corresponding to \mathcal{E}_2 in Eq. (13) is then given by

$$\int_{d^*}^\infty \int_0^{\theta_0(d, d^*)} P(L^{*,b} \leq l_0(d, d^*, \theta)) \frac{2}{\pi} f_D(d) d\theta dd. \quad (34)$$

Case 3. Our last case corresponds to Figure 4(c) and the integral term corresponding to event \mathcal{E}_3 in Eq. (13) where given d, d^* and $\theta \leq \theta_0(d, d^*)$ we have

$$L^{*,b} > l_0(d, d^*, \theta) \quad (35)$$

i.e., the vehicle cluster extends into the circle \mathcal{C}_1 of radius d^* . In order for $D^* > d^*$ all vehicles within the circle must be closer to another BS than that at the origin.

The situation is illustrated in Figure 4(d) where we draw two other circles. The first is \mathcal{C}_2 is centered on the first (starting

from our typical vehicle at $(d, 0)$) cluster vehicle that lies within \mathcal{C}_1 and has a radius given by its distance to the origin, i.e., base station b . The second, \mathcal{C}_3 is centered at the typical vehicle $(d, 0)$ and has radius d , i.e. also crosses the origin. Recalling that b is the closest base station to the vehicle at $(d, 0)$, and thus \mathcal{C}_3 contains no other base stations, a necessary and sufficient condition to ensure that no cluster vehicle within \mathcal{C}_1 is associated with base station b is that there is at least one BS in the shaded region $\mathcal{R}(d, d^*, \theta)$ representing all locations that are closer to the first vehicle in \mathcal{C}_1 than to b . This follows because

- if there is a BS in $\mathcal{R}(d, d^*, \theta)$ then not only will the first cluster vehicle in \mathcal{C}_1 not be associated with b , but so will all the others, since the circle centered on each such vehicle and traversing the origin, will contain $\mathcal{R}(d, d^*, \theta)$. We can then conclude that $D^* > d^*$.
- if $\mathcal{R}(d, d^*, \theta)$ is empty, then at least one vehicle in the cluster is less than d^* meters away from b , i.e. $D^* \leq d^*$.

Using basic algebra and the law of cosines one can show that the distance between the typical vehicle and the first cluster vehicle in \mathcal{C}_1 is given by

$$d_f(d, d^*, \theta) := d_v \cdot \left[\frac{l_0(d, d^*, \theta)}{d_v} \right]$$

and the distance from the first vehicle to the origin (i.e., radius of \mathcal{C}_2) is given by

$$r_2(d, d^*, \theta) := \sqrt{d^2 + d_f^2 - 2d \cdot d_f \cos(\theta)}. \quad (36)$$

where we have suppressed the arguments of $d_f(\cdot, \cdot)$.

Using the expression in [31] for the area of $\mathcal{C}_2 \cap \mathcal{C}_3$, as a function of d, d_f and r_2 , one can find an expression for the area of $\mathcal{R}(d, d^*, \theta)$:

$$a(d, d^*, \theta) = \pi r_2^2 - \left[r_2^2 \cos^{-1}\left(\frac{d_f^2 + r_2^2 - d^2}{2d_f r_2}\right) + d^2 \cos^{-1}\left(\frac{d_f^2 + d^2 - r_2^2}{2d_f d}\right) - \frac{\sqrt{(-d_f + r_2 + d)(d_f + r_2 - d)(d_f - r_2 + d)(d_f + r_2 + d)}}{2} \right] \quad (37)$$

where we have suppressed the arguments of $d_f(\cdot, \cdot)$ and $r_2(\cdot, \cdot)$.

Since BS form a PPP, the probability there is at least one base station in \mathcal{R} is given by

$$e(d, d^*, \theta) := P(\Phi_B \cap \mathcal{R}(d, d^*, \theta) \neq \emptyset) = 1 - e^{-\lambda_{BS} a(d, d^*, \theta)}.$$

The third integral term in Eq. (13) corresponding to \mathcal{E}_3 is then given by

$$\int_{d^*}^\infty \int_0^{\theta_0(d^*, d)} P(L^{*,b} > l_0(d, d^*, \theta)) e(d, d^*, \theta) \frac{2}{\pi} f_D(d) d\theta dd \quad (38)$$

The distribution of D^* can now be determined, along with an expression for the expected typical user peak rate $\mathbb{E}[R^*]$ similarly as the non-cooperative scenario using Eq. (10). The bound comes from the fact that the closest vehicle from the BS sees less interference than the typical vehicle, as we know that there are no BSs in \mathcal{C}_3 . \square